Robust Local Bootstrap for Weakly Stationary Time Series in the Presence of Additive Outliers

Carlo Corrêa Solci[1], Valdério Anselmo Reisen[1,2,3*†] and Paulo Canas Rodrigues[4†]

[1]Post-Graduation Program in Environmental Engineering, Federal University of Espírito Santo, Vitória, Espírito Santo, Brazil.
[2*]Laboratoire des Signaux et Systèmes (L2S), CNRS-CentraleSupélec-Université Paris-Sud, Gif-sur-Yvette, France.
[3]Post-Graduation Program in Statistics, Federal University of Minas Gerais, Belo Horizonte, Minas Gerais, Brazil.
[4]Department of Statistics, Federal University of Bahia, Salvador, Bahia, Brazil.

*Corresponding author(s). E-mail(s): valderioanselmoreisen@gmail.com;
Contributing authors: csolci13@gmail.com; paulocanas@gmail.com;
†These authors contributed equally to this work.

Abstract

The aim of this paper is to propose a generalization of the local bootstrap for periodogram statistics to the case when weakly stationary time series are contaminated by additive outliers. In order to achieve robustness, we suggest to replace the classical version of the periodogram with the M-periodogram in the local bootstrap procedure. The robust bootstrap periodogram is implemented in the Whittle estimator to obtain confidence intervals for the parameters of a time series model. A finite sample size investigation was conducted to compare the performance of the classical local bootstrap with the one proposed in this paper, to estimate 95% confidence intervals for the parameters of autoregressive and of seasonal autoregressive time series. The results have shown that the robust estimator is resistant to additive outlier contamination and produces confidence intervals with coverage percentage closer to 95% and with lower amplitudes than the ones obtained with the classical estimator, even for small percentages and magnitudes of outliers. It was also empirically demonstrated that when the expected number of outliers is kept constant, the coverage percentages of the confidence intervals of the robust estimators tend to 95% as the sample size increases. An application to the daily mean concentration of the particulate matter with diameter smaller than 10 µm (PM_{10}) was considered to illustrate the methodologies in a real data context. All the results presented here give strong motivation to use the proposed robust methodology in practical situations in which weakly stationary time series are contaminated by additive outliers.

Keywords: Bootstrap; Periodogram; Robust estimation; Whittle estimator; PM_{10} pollutant.

1 Introduction

The bootstrap is a resampling technique that provides tools for statistical analysis without requiring rigorous structural assumptions. It was initially proposed by Efron (1979), but despite its efficiency for independent and identically distributed (i.i.d.) variables, it was shown by Singh (1981) that Efron's methodology is inadequate to the case of dependent data. Due to this fact, several approaches to perform the bootstrap in time series have been proposed, as addressed, for example in Lahiri (2003) and Kreiss and Paparoditis (2011). In time series, the bootstrap approaches can be built in the time and frequency domains.

As well-known, an important quantity for time series analysis in the frequency domain is the spectral density function which can be estimated classically by the periodogram, hence the bootstrap in this domain generates periodogram replicates. In this context, the bootstrap in the frequency domain has an advantage over the one in the time domain since, for weakly stationary processes, the periodogram ordinates are nearly independent (a more precise definition is that they are asymptotically independent). Thus, the classical bootstrap approach of drawing with replacement of Efron (1979) can be potentially applied to them. There are several bootstrap approaches in the frequency domain, some examples are the multiplicative residual bootstrap of Franke and Härdle (1992), the local bootstrap of Paparoditis and Politis (1999) and the hybrid bootstrap of Kreiss and Paparoditis (2003).

The bootstrap methodologies in the frequency domain are useful to estimate population quantities, such as the standard error and the quantiles of some statistic of interest, based on the sampling distribution of estimators that are functions of the periodogram. Among these approaches, a particularly interesting one is the local bootstrap of Paparoditis and Politis (1999) because of its simplicity to implement and its similarity to the approach of Efron (1979). Due the fact that the distribution of each periodogram ordinate is a function of its frequency, the resampling is performed locally, that is, by choosing with replacement between periodogram ordinates corresponding to frequencies which are near to the frequency of interest.

In order to use the local bootstrap to obtain confidence intervals of the parameter vector $\boldsymbol{\varphi}$ of weakly stationary time series models, it is necessary to estimate the values of these parameters as functionals of the periodogram $I_N(\lambda)$ of a sample $Y_1, Y_2 \ldots, Y_N$, as well as of the parametric spectral density $f(\lambda, \boldsymbol{\varphi})$ of the process $\{Y_t\}$, $t \in \mathbb{Z}$. This can be achieved by using an important class of estimators that are obtained through the minimization of the criterion $\int_{-\pi}^{\pi} \left\{ \log f(\lambda, \boldsymbol{\varphi}) + \frac{I_N(\lambda)}{f(\lambda, \boldsymbol{\varphi})} \right\} d\lambda$, which are well-known as the Whittle estimators and were initially proposed by Whittle (1953). The confidence intervals of $\boldsymbol{\varphi}$, computed by using local bootstrap, are obtained without having to make parametric assumptions about the form of the underlying population $\{Y_t\}$. This makes the local bootstrap an interesting alternative to estimate confidence intervals of the parameters of weakly stationary time series models.

It is important to recall that, since the periodogram is a classical estimator of the spectral density function, it does not have the property of being resistant to additive outlier contamination. Hence, the Whittle estimators have their performance deteriorated when there is presence of this kind of observation. In this situation it is more appropriate to use a robust version of the Whittle estimators which is obtained by replacing the periodogram $I_N(\lambda)$ in the criterion $\int_{-\pi}^{\pi} \left\{ \log f(\lambda, \boldsymbol{\varphi}) + \frac{I_N(\lambda)}{f(\lambda, \boldsymbol{\varphi})} \right\} d\lambda$ by a robust counterpart of $I_N(\lambda)$. In this context, there are some versions of the periodogram that are resistant to additive outlier contamination such as the Q_n-periodogram, see, for example, Molinares et al (2009), and the M-periodogram, see, for instance, Reisen et al (2017); Fajardo et al (2018). The latter has the advantage to provide an autocovariance function which is positive semidefinite and this motivates the use of the robust version of the Whittle estimators obtained by using it as the estimator of the spectral density function. Since the methodology proposed by Paparoditis and Politis (1999) is based in the resampling of the ordinates of the classical periodogram $I_N(\lambda)$ to obtain via Whittle estimators the bootstrap confidence intervals of the parameters of weakly stationary time series, these intervals are shifted to the left when there is contamination by additive outliers because of the sensitivity of $I_N(\lambda)$ to this type of outlying observation.

In this context, this paper proposes a robust alternative to the local bootstrap of Paparoditis and Politis (1999) which is resistant to additive outlier contamination since it generates confidence intervals of parameters of weakly stationary time series with a significant reduction in the aforementioned effect of left shift. The proposed robust local bootstrap is obtained by replacing the classical periodogram $I_N(\lambda)$ by the robust M-periodogram $I_{N,\psi}(\lambda)$ of Reisen et al (2017). Hence, the bootstrap versions of the time series parameters are obtained via the robust Whittle estimator that uses $I_{N,\psi}(\lambda)$. The finite sample properties of the robust local bootstrap for series generated by the processes AR(1) and SARMA$(1,0) \times (1,0)_4$ under scenarios with and without additive outlier contamination were investigated and compared to the ones of the methodology of Paparoditis and Politis (1999) through a Monte Carlo study. Furthermore, the daily mean concentration of the atmospheric pollutant PM_{10} (particulate matter with diameter smaller than 10 µm) in the Great Vitória Region, in the Brazilian state of Espírito Santo, was used to illustrate the bootstrap methodologies in a real air quality area application, because it may present observations with high levels of pollutant concentrations which can be modeled as additive outliers.

The rest of the paper is organized as follows: Section 2 summarizes the well-known local bootstrap of Paparoditis and Politis (1999) and shows how to compute the classical periodogram based on a regression equation, it also discusses the robust M-periodogram of Reisen et al (2017) and its asymptotic properties; Section 3 introduces the proposed robust local bootstrap and discusses the Whittle estimator and its robust counterpart that uses $I_{N,\psi}(\lambda)$; Section 4 presents the results of the Monte Carlo simulation experiment; Section 5 shows the results of the application of the bootstrap methodologies to PM_{10} concentrations; Section 6 concludes the paper.

2 The Model, Assumptions, the Local Bootstrap and Spectral Estimators

Let $\{Y_t\}$, $t \in \mathbb{Z}$, be a real valued weakly stationary linear process, i.e., it satisfies the difference equation

$$Y_t = \sum_{j=-\infty}^{\infty} \psi_j \epsilon_{t-j}, \tag{1}$$

where $\{\epsilon_t\}$, $t \in \mathbb{Z}$, is a sequence of i.i.d. random variables with $\mathsf{E}(\epsilon_t) = 0$, $\mathsf{E}(\epsilon_t^2) = \sigma^2$ and $\mathsf{E}(\epsilon_t^4) < \infty$. Moreover, $\{\psi_j\}$, $j \in \mathbb{Z}$, is a sequence of constants such that $\psi_0 = 1$ and $\sum_{j=-\infty}^{\infty} |\psi_j| < \infty$.

Since the robust local bootstrap approach proposed in this paper is based on the local bootstrap method suggested in Paparoditis and Politis (1999), some of their assumptions are also considered here.

Let $Y_1, Y_2, \ldots, Y_N$, be a sample from the process $\{Y_t\}$ and $\lambda_j = 2\pi j/N$, $j = 0, 1, 2, \ldots, N'$, be the Fourier frequencies with $N' = [N/2]$, where $[x]$ is the integer part of x. A classical non-parametric spectral estimator is the periodogram function which is given by

$$I_N(\lambda_j) = \frac{1}{2\pi N} \left| \sum_{t=1}^{N} Y_t \exp(-i\lambda_j t) \right|^2. \tag{2}$$

This definition can be extended for any $\lambda \in [-\pi, \pi]$, if we let $I_N(\lambda) = I_N\{r(N, \lambda)\}$, where for $\lambda \in [0, \pi]$ we have that $r(N, \lambda)$ is the multiple of $2\pi/N$ closest to λ (the smaller one if there are two), and for $\lambda \in [-\pi, 0)$ we set $r(N, \lambda) = r(N, -\lambda)$.

The local bootstrap procedure relies on the asymptotic independence of the periodogram ordinates as well as in the smoothness of the spectral density function. To achieve these necessary properties, $f(\lambda)$ has to fulfill the following conditions.

Remark 1 If the spectral density of Y_t in (1), obtained by $f(\lambda) = \sigma^2(2\pi)^{-1}\left|\sum_{j=-\infty}^{\infty}\psi_j \exp(-ij\lambda)\right|^2$, satisfies $f(\lambda) > 0$ for all $\lambda \in [-\pi, \pi]$, and if $0 < \lambda_1 < \cdots < \lambda_m < \pi$, then the random vector $(I_N(\lambda_1), \ldots, I_N(\lambda_m))'$ converges in distribution to a vector of independent and exponentially distributed random variables, the i^{th} component of which has mean $f(\omega_i)$, $i = 1, \ldots, m$. Under the additional assumption of $\sum_{j=-\infty}^{\infty} |j|^{1/2} |\psi_j| < \infty$, we have that $\mathsf{Cov}(I_N(\lambda_j), I_N(\lambda_k)) = O(N^{-1})$, if $\lambda_j \neq \lambda_k$. In order to ensure the smoothness of the spectral density we assume that $f(\lambda)$ is continuously differentiable with bounded derivative in $[-\pi, \pi]$.

The asymptotic results in Remark 1 show that the periodogram, although is an unbiased estimator of the spectral density, it is not a consistent estimator, i.e, its variance $\mathsf{Var}(I_N(\lambda_j)) = O(1)$ (as $N \to \infty$). However, for any two neighboring frequencies, λ_1, λ_2, $\mathsf{Cov}(I_N(\lambda_1), I_N(\lambda_2))$ decreases as N increases. With the assumptions that the errors $\{\epsilon_t\}$ are Gaussian white noise processes and $\sum_{j=-\infty}^{\infty} |\psi_j| < \infty$, we have that asymptotically the set of random variables $\{2I_N(\lambda_j)/f(\lambda_j)\}$, $j = 0, 1, \ldots, N'$, are independently distributed, and for $j \neq 0, N/2$ (N even), each is asymptotically distributed as a $\chi^2_{(2)}$.

The local bootstrap scheme for the periodogram is summarized as follows (for more details, see Paparoditis and Politis (1999)).

(i) Choose a resampling width k_N where $k_N = k(N) \in \mathbb{N}$ and $k_N \leq [N'/2]$.

(ii) Define i.i.d. discrete random variables $J_1, J_2, \ldots, J_{N'}$, that assume values in the set $\{-k_N, -k_N + 1, \ldots, k_N\}$ with probability $\mathsf{P}(J_i = s) = p_{k_N,s}$ for $s = 0, \pm 1, \ldots, \pm k_N$.

(iii) The bootstrap periodogram can be defined by $I_N^*(\lambda_j) = I_N(\lambda_{J_j+j})$ for $j = 1, 2, \ldots, N'$, $I_N^*(\lambda_j) = I_N^*(-\lambda_j)$ for $\lambda_j < 0$ and for $\lambda_j = 0$ we have $I_N^*(\lambda_j) = 0$.

Conditionally on the sample $Y_1, Y_2, \ldots, Y_N$, the expected value and variance of the bootstrap periodogram are, respectively, given by

$$\mathsf{E}\{I_N^*(\lambda)|Y_1, Y_2, \ldots, Y_N\} = \sum_{s=-k_N}^{k_N} p_{k_N,s} I_N\{r(N,\lambda) + \lambda_s\} \equiv \tilde{f}(\lambda) \qquad (3)$$

and

$$\mathsf{Var}\{I_N^*(\lambda|Y_1, Y_2, \ldots, Y_N)\} = \sum_{s=-k_N}^{k_N} p_{k_N,s} I_N^2\{r(N,\lambda) + \lambda_s\} - \tilde{f}^2(\lambda). \qquad (4)$$

As can be seen from Equations 3 and 4, $\tilde{f}(\lambda)$ and $\sum_{s=-k_N}^{k_N} p_{k_N,s} I_N^2\{r(N,\lambda) + \lambda_s\}$ can be thought of as kernel estimators of $f(\lambda)$ and $\mathsf{E}\{I_N^2(\lambda)\} = \{2 + \eta(\lambda)\} f^2(\lambda) + o(1)$, respectively, where

$$\eta(\lambda) = \begin{cases} 1, & \text{if } \lambda = 0 \,(\mathrm{mod}\, \pi)\,, \\ 0, & \text{otherwise.} \end{cases}$$

Thus, in order to ensure the convergence of $I_N^*(\lambda)$, we need to let $k_N \to \infty$ as $N \to \infty$ such that $k_N = \mathrm{o}(N)$, and the sequence $\{p_{k_N,s} : -k_N \le s \le k_N\}$ has to satisfy $\sum_{s=-k_N}^{k_N} p_{k_N,s} = 1$, $p_{k_N,s} = p_{k_N,-s}$ and $\sum_{s=-k_N}^{k_N} p_{k_N,s}^2 \to 0$ as $k_N \to \infty$.

Under the above assumption, it follows that, in probability, $\mathsf{E}\{I_N^*(\lambda)|Y_1, Y_2, \ldots, Y_N\} \to f(\lambda)$ and $\mathsf{Var}\{I_N^*(\lambda|Y_1, Y_2, \ldots, Y_N)\} \to (1 + \eta(\lambda)) f^2(\lambda)$. These show that, for a fixed j and for $N \to \infty$, the bootstrap periodogram $I_N^*(\lambda_j)$ has the same mean and variance of $I_N(\lambda_j)$. The authors also established that $I_N^*(\lambda_j) \to I_N(\lambda_j)$ in distribution.

In practical situations, $p_{k_N,s}$ is chosen based on

$$p_{k_N,s} = \frac{W(\pi s k_N^{-1})}{\sum_{s=-k_N}^{k_N} W(\pi s k_N^{-1})}, \tag{5}$$

where $W(\cdot)$ is a sequence of weight functions satisfying, for all λ, $W(\lambda) = W(-\lambda)$, $W(\lambda) \geq 0$, and $\int_{-\pi}^{\pi} W(\lambda)d\lambda = 1$, $\int_{-\pi}^{\pi} W^2(\lambda)d\lambda < \infty$. $W(\cdot)$ is well-known as a kernel function, and is widely used to obtain a consistent spectral estimator, i.e, the smoothed periodogram. Classical examples of $W(\cdot)$ are: Parzen kernel, Daniell kernel, Bartlett-Priestley kernel, among others (see, for instance, Taniguchi and Kakizawa (2000); Priestley (1981) for further details).

Alternatively, when comparing the results of the local bootstrap applied to samples with different sizes it may be more convenient to fix constants $\nu > 0$ and $\alpha \in (0,1)$ in order to define a resampling bandwidth $b_N = \nu N^{-\alpha}$ as a function of N and calculate the corresponding resampling width as $k_N = [N b_N/2]$. This yields an alternative version of (5) which is given by

$$p_{b_N,s} = \frac{W\{2\pi s (N b_N)^{-1}\}}{\sum_{s=-k_N}^{k_N} W\{2\pi s (N b_N)^{-1}\}}.$$

As addressed, for example, in Reisen et al (2017); Fajardo et al (2018), the periodogram in (2) can also be computed based on the following regression equation

$$Y_i = c'_{Ni}\boldsymbol{\beta} + \varepsilon_i = \beta^{(1)}\cos(i\lambda_j) + \beta^{(2)}\sin(i\lambda_j) + \varepsilon_i\ ,\ 1 \leq i \leq N,\ \boldsymbol{\beta} \in \mathbb{R}^2\ , \tag{6}$$

where $\boldsymbol{\beta} = (\beta^{(1)}, \beta^{(2)})$ and ε_i denotes the deviation of Y_i from $c'_{Ni}\boldsymbol{\beta}$. Thus, the periodogram $I_N(\lambda_j)$ is calculated from

$$I_N(\lambda_j) = \frac{N}{8\pi}\|\hat{\boldsymbol{\beta}}_N^{\mathrm{LS}}(\lambda_j)\|^2 = \frac{N}{8\pi}\left((\hat{\beta}_N^{\mathrm{LS},(1)}(\lambda_j))^2 + (\hat{\beta}_N^{\mathrm{LS},(2)}(\lambda_j))^2\right) =: I_N^{\mathrm{LS}}(\lambda_j), \tag{7}$$

where $\|\cdot\|$ denotes the classical Euclidian norm and $\hat{\boldsymbol{\beta}}_N^{\mathrm{LS}}(\lambda_j) = (\hat{\beta}_N^{\mathrm{LS},(1)}(\lambda_j), \hat{\beta}_N^{\mathrm{LS},(2)}(\lambda_j))'$ is the least-square estimator of $\boldsymbol{\beta} = (\beta^{(1)}, \beta^{(2)})$ in the linear regression model given in (6) computed from

$$\hat{\boldsymbol{\beta}}_N^{\mathrm{LS}}(\lambda_j) = \underset{\boldsymbol{\beta}(\lambda_j)\in\mathbb{R}^2}{\operatorname{argmin}} \sum_{i=1}^{N}(Y_i - c'_{N,i}(\lambda_j)\boldsymbol{\beta}(\lambda_j))^2, \tag{8}$$

where

$$c'_{N,i}(\lambda_j) = (\cos(i\lambda_j)\ \sin(i\lambda_j)). \tag{9}$$

2.1 The M-periodogram Spectral Estimator

As it is well-known, M-estimation is an alternative robust procedure to the least-square estimation approach. Thus, based on the regression equation in (6), the M-regression estimator is used here to estimate the vector $\boldsymbol{\beta} = (\beta^{(1)}, \beta^{(2)})$ by $\hat{\boldsymbol{\beta}}_{N,\psi}(\lambda_j) = (\hat{\beta}^{(1)}_{N,\psi}(\lambda_j), \hat{\beta}^{(2)}_{N,\psi}(\lambda_j))$, which is the solution of

$$\sum_{i=1}^{N} c_{N,i}(\lambda_j)\psi(Y_i - c'_{N,i}(\lambda_j)\hat{\boldsymbol{\beta}}_{N,\psi}(\lambda_j)) = \mathbf{0}, \tag{10}$$

where $\psi(\cdot)$ was chosen as the Huber (1964) function,

$$\psi(x) = \psi_\delta(x) = \begin{cases} x, & \text{if } |x| \le \delta, \\ \operatorname{sign}(x)\delta, & \text{if } |x| > \delta. \end{cases} \tag{11}$$

By analogy to (7), the robust periodogram $I_{N,\psi}(\lambda_j)$ is defined by

$$I_{N,\psi}(\lambda_j) = \frac{N}{8\pi}\|\hat{\boldsymbol{\beta}}_{N,\psi}(\lambda_j)\|^2 = \frac{N}{8\pi}\left[(\hat{\beta}^{(1)}_{N,\psi}(\lambda_j))^2 + (\hat{\beta}^{(2)}_{N,\psi}(\lambda_j))^2\right]. \tag{12}$$

Similarly to $I_N(\lambda)$, this definition can also be extended for any $\lambda \in [-\pi, \pi]$, if we let $I_{N,\psi}(\lambda) = I_{N,\psi}\{r(N,\lambda)\}$ for $\lambda \in [0,\pi]$ and for $\lambda \in [-\pi, 0)$ we set $r(N,\lambda) = r(N,-\lambda)$.

Remark 2 The Huber function is chosen here because it satisfies assumptions (A1)-(A4) of Reisen et al (2019). These authors establish that, for any fixed j and under the additional assumption that $\varepsilon_i = \sum_{j=0}^{\infty} a_j \eta_{i-j}$, where $\{\eta_j\}$, $j \in \mathbb{Z}$, is a sequence of i.i.d. standard Gaussian random variables as well as that a_j is a sequence of constants such that $a_0 = 1$ and $\sum_{j=0}^{\infty}|a_j| < \infty$, we have

$$I_{N,\psi}(\lambda_j) \xrightarrow{d} \frac{X^2 + Y^2}{4\pi(F(c) - F(-c))^2}, \quad \text{as } N \to \infty, \tag{13}$$

where c is a positive constant, $F(\cdot)$ is the cumulative distribution function of ε_1,

$$X \sim \mathcal{N}\left(0, \sum_{k\in\mathbb{Z}} \mathsf{E}\{\psi(\varepsilon_0)\psi(\varepsilon_k)\}\cos(k\lambda_j)\right), \; Y \sim \mathcal{N}\left(0, \sum_{k\in\mathbb{Z}} \mathsf{E}\{\psi(\varepsilon_0)\psi(\varepsilon_k)\}\cos(k\lambda_j)\right) \tag{14}$$

and

$$\mathsf{Cov}(X,Y) = \sum_{k\in\mathbb{Z}} \mathsf{E}\{\psi(\varepsilon_0)\psi(\varepsilon_k)\}\sin(k\lambda_j). \tag{15}$$

As well-addressed in the recent literature, the M-periodogram $I_{N,\psi}(\cdot)$ becomes an alternative spectral estimator for linear time series, with short- and long-memory correlation structures, such as ARMA and ARFIMA processes, respectively. An overview of robust spectral estimators for these classes of time series is addressed in Reisen et al (2019). In addition to its elegant asymptotic properties, $I_{N,\psi}(\cdot)$ has the interesting empirical property of being robust against outliers, while the classical periodogram $I_N(\cdot)$ of (7) is fully affected by this type of observations.

3 The Local Bootstrap and Whittle Estimator Using $I_{N,\psi}(\cdot)$

We now introduce the local bootstrap using $I_{N,\psi}(\cdot)$, denoted by $I^*_{N,\psi}(\cdot)$. This approach follows similar guidelines of the local bootstrap scheme discussed previously where k_N, b_N, W, $\{p_{k_N,s} : -k_N \leq s \leq k_N\}$, $\{p_{b_N,s} : -k_N \leq s \leq k_N\}$, $\{I_N(\lambda_j) : 0 \leq j \leq N'\}$, and $\{I^*_N(\lambda_j) : 0 \leq j \leq N'\}$ are replaced by $k_{N,\psi}$, $b_{N,\psi}$, W_ψ, $\{p_{k_{N,\psi},s'} : -k_{N,\psi} \leq s' \leq k_{N,\psi}\}$, $\{p_{b_{N,\psi},s'} : -k_{N,\psi} \leq s' \leq k_{N,\psi}\}$, $\{I_{N,\psi}(\lambda_j) : 0 \leq j \leq N'\}$, and $\{I^*_{N,\psi}(\lambda_j) : 0 \leq j \leq N'\}$, respectively. The assumptions for $k_{N,\psi}$, W_ψ, and $\{p_{k_{N,\psi},s'} : -k_{N,\psi} \leq s' \leq k_{N,\psi}\}$ are kept the same as of k_N, W, and $\{p_{k_N,s} : -k_N \leq s \leq k_N\}$, sequentially. Without loss of generality, we assume here that $k_{N,\psi} = k_N$, $b_{N,\psi} = b_N$, $W_\psi = W$, $\{p_{k_{N,\psi},s'} : -k_{N,\psi} \leq s' \leq k_{N,\psi}\} = \{p_{k_N,s} : -k_N \leq s \leq k_N\}$, and $\{p_{b_{N,\psi},s'} : -k_{N,\psi} \leq s' \leq k_{N,\psi}\} = \{p_{b_N,s} : -k_N \leq s \leq k_N\}$.

Analogously to the local bootstrap for the classical periodogram, the first two conditional moments of the robust bootstrap periodogram $I^*_{N,\psi}(\lambda)$ are, respectively, given by

$$\mathsf{E}\{I^*_{N,\psi}(\lambda)|Y_1, Y_2, \ldots, Y_N\} = \sum_{s'=-k_{N,\psi}}^{k_{N,\psi}} p_{k_{N,\psi},s'} I_{N,\psi}\{r(N,\lambda) + \lambda_{s'}\} \equiv \tilde{f}_\psi(\lambda) \tag{16}$$

and

$$\mathsf{Var}\{I^*_{N,\psi}(\lambda|Y_1, Y_2, \ldots, Y_N)\} = \sum_{s'=-k_{N,\psi}}^{k_{N,\psi}} p_{k_{N,\psi},s'} I^2_{N,\psi}\{r(N,\lambda) + \lambda_{s'}\} - \tilde{f}^2_\psi(\lambda). \tag{17}$$

It is important to emphasize that $\tilde{f}_{\psi}(\lambda)$ and $\sum_{s'=-k_{N,\psi}}^{k_{N,\psi}} p_{k_{N,\psi},s'} I^2_{N,\psi}\{r(N,\lambda)+\lambda_{s'}\}$ can be thought of as robust kernel estimators of $f(\lambda)$ and $\mathsf{E}\{I^2_N(\lambda)\}$, respectively.

3.1 Whittle Estimators

To estimate the parameters of the model satisfying Equation 1, we consider the Whittle estimator initially proposed by Whittle (1953) and widely used in the literature of time series. Let $\boldsymbol{\varphi}$ be the parameter vector of the process $\{Y_t\}$ with parametric spectral density $f(\lambda, \boldsymbol{\varphi})$. The estimates of $\boldsymbol{\varphi}$, denoted by $\hat{\boldsymbol{\varphi}}_W$, are obtained by minimizing

$$\int_{-\pi}^{\pi} \left\{ \log f(\lambda, \boldsymbol{\varphi}) + \frac{I_N(\lambda)}{f(\lambda, \boldsymbol{\varphi})} \right\} d\lambda, \tag{18}$$

where the notation log refers to the natural logarithm and $I_N(\lambda)$ is the periodogram function defined previously and computed from the sample $Y_1, \ldots, Y_N$, of the process $\{Y_t\}$. Equivalently, the Whittle estimator $\hat{\boldsymbol{\varphi}}_W$ can be obtained by minimizing

$$\bar{\sigma}^2_N(\boldsymbol{\varphi}) = \frac{1}{N} \sum_j \frac{I_N(\lambda_j)}{g(\lambda_j, \boldsymbol{\varphi})} \tag{19}$$

where $g(\lambda, \boldsymbol{\varphi}) = 2\pi f(\lambda, \boldsymbol{\varphi})/\sigma^2$ and the sum is taken over all frequencies $\lambda_j = 2\pi j/N \in (-\pi, \pi]$.

The classical weakly stationary and invertible Autoregressive Moving Average (ARMA(p,q)) model $Y_t - \phi_1 Y_{t-1} - \cdots - \phi_p Y_{t-p} = \epsilon_t - \theta_1 \epsilon_{t-1} - \cdots - \theta_q \epsilon_{t-q}$, $\{\epsilon_t\} \sim \text{IID}(0, \sigma^2)$ and $\mathsf{E}(\epsilon_t^4) < \infty$, where $\phi(z) = 1 - \phi_1 z - \cdots - \phi_p z^p$ and $\theta(z) = 1 - \theta_1 z - \cdots - \theta_q z^q$ have no common zeroes, is a particular time series model satisfying Equation 1. For this model, we have $g(\lambda, \boldsymbol{\varphi}) = \left|\theta(e^{-i\lambda})\right|^2 / \left|\phi(e^{-i\lambda})\right|^2$.

Remark 3 Let $\boldsymbol{\varphi} = (\phi_1, \ldots, \phi_p, \theta_1, \ldots, \theta_q)'$ and denote by C the parameter set, $C = \{\boldsymbol{\varphi} \in \mathbb{R}^{p+q} : \phi(z)\theta(z) \neq 0$ for $|z| \leq 1$, $\phi_p \neq 0$, $\theta_q \neq 0$, and $\phi(\cdot)$, $\theta(\cdot)$ have no common zeroes$\}$. Let $\bar{\boldsymbol{\varphi}}_N$ be the estimator in C that minimizes $\bar{\sigma}_N^2(\boldsymbol{\varphi})$ for an ARMA process $\{Y_t\}$ with true parameter values $\boldsymbol{\varphi}_0 \in C$ and $\sigma_0^2 > 0$. Then,

(i) $\bar{\boldsymbol{\varphi}}_N \xrightarrow{as} \boldsymbol{\varphi}_0$ and $\bar{\sigma}_N(\bar{\boldsymbol{\varphi}}_N) \xrightarrow{as} \sigma_0^2$, as $N \to \infty$, where $\xrightarrow{as}$ denotes almost sure convergence.

(ii) $\bar{\boldsymbol{\varphi}}_N \xrightarrow{d} \mathcal{N}(\boldsymbol{\varphi}_0, N^{-1}V^{-1}(\boldsymbol{\varphi}_0))$, as $N \to \infty$, where

$$V(\boldsymbol{\varphi}_0) = \frac{1}{4\pi}\int_{-\pi}^{\pi}\left[\frac{\partial \log g(\lambda, \boldsymbol{\varphi}_0)}{\partial \boldsymbol{\varphi}}\right]\left[\frac{\partial \log g(\lambda, \boldsymbol{\varphi}_0)}{\partial \boldsymbol{\varphi}}\right]' d\lambda,$$

with $\xrightarrow{d}$ denoting convergence in distribution.

The results of items (i) and (ii) are stated in Theorems 10.8.1 and 10.8.2 of Brockwell and Davis (1991), respectively.

(iii) Replacing $I_N(\lambda_j)$ by $I_{N,\psi}(\lambda_j)$ in Equation 19, it is possible to obtain the Whittle estimator of $\boldsymbol{\varphi}$ using M-periodogram, i.e, $\hat{\boldsymbol{\varphi}}_{W,\psi}$, by minimizing

$$\bar{\sigma}_{N,\psi}^2(\boldsymbol{\varphi}) = \frac{1}{N}\sum_j \frac{I_{N,\psi}(\lambda_j)}{g(\lambda_j, \boldsymbol{\varphi})}, \tag{20}$$

where the sum is also taken over all frequencies $\lambda_j = 2\pi j/N \in (-\pi, \pi]$.

(iv) It can be shown that

$$\hat{\boldsymbol{\varphi}}_{W,\psi} \xrightarrow{p} \boldsymbol{\varphi}_0, \text{ as } N \to \infty, \tag{21}$$

where $\xrightarrow{p}$ denotes convergence in probability. The proof of the above result follows similar arguments of Theorem 10.8.1 in Brockwell and Davis (1991).

Regarding the local bootstrap estimators discussed here, $\hat{\boldsymbol{\varphi}}_W^*$ is obtained by replacing $I_N(\lambda_j)$ by $I_N^*(\lambda_j)$ in (19), while one can get $\hat{\boldsymbol{\varphi}}_{W,\psi}^*$ by replacing $I_{N,\psi}(\lambda_j)$ by $I_{N,\psi}^*(\lambda_j)$ in (20). Whereas concerning the conditional expected values of these estimators, $\tilde{\boldsymbol{\varphi}}_W = \mathsf{E}(\hat{\boldsymbol{\varphi}}_W^*|Y_1, Y_2, \ldots, Y_N)$ can be calculated by replacing $I_N(\lambda_j)$ by $\tilde{f}(\lambda_j)$ in (19) while one can obtain $\tilde{\boldsymbol{\varphi}}_{W,\psi} = \mathsf{E}(\hat{\boldsymbol{\varphi}}_{W,\psi}^*|Y_1, Y_2, \ldots, Y_N)$ by replacing $I_{N,\psi}(\lambda_j)$ by $\tilde{f}_\psi(\lambda_j)$ in (20). The empirical properties of these estimators are discussed in the next section.

4 Monte Carlo Study

In order to investigate the impact of atypical observations on the estimates obtained from the methods discussed previously, series of weakly stationary linear processes were generated with and without outliers. Let $\{Z_t\}$ be defined as follows

$$Z_t = Y_t + \omega V_t \tag{22}$$

where $\{Y_t\}$ is a weakly stationary linear process that satisfies Equation 1, additionally, $\{V_t\}$ is a sequence of independent random variables with $\mathsf{P}(V_t = -1) = \mathsf{P}(V_t = 1) = \xi/2$ and $\mathsf{P}(V_t = 0) = 1 - \xi$, $\xi \in (0, 1)$. Moreover, for all t and s, $\{Y_t\}$ and $\{V_s\}$ are independent variables and ω is the magnitude of the outlier.

The simulation study was carried out via the generation of series of autoregressive and seasonal autoregressive processes with and without additive outliers. More specifically, the time series chosen were of AR(1) $Y_t = \phi Y_{t-1} + \epsilon_t$ with $\phi = 0.2$, 0.5, and 0.8, as well as of SARMA$(1, 0) \times (1, 0)_{\mathcal{S}}$ processes $Y_t = \phi Y_{t-1} + \Phi Y_{t-\mathcal{S}} - \phi\Phi Y_{t-\mathcal{S}-1} + \epsilon_t$ with $\mathcal{S} = 4$, $\phi = 0.5$, and $\Phi = 0.2$, 0.5, and 0.7. The series $\{Y_t\}$ of both processes were contaminated by additive outliers according to Equation 22 with $pr_{out} = \xi = 0.005$ and 0.01, and $\omega = 0$, 4, and 7, generating the processes $\{Z_t\}$. The parameter values were chosen to achieve stationarity and low, moderate and strong correlation dependency. The sample sizes were taken as small ($N = 200$) and large ($N = 400$), which are common sample sizes in practical situations, and for the series of both processes the random variables ϵ_t were generated independently and $\mathcal{N}(0, 1)$ distributed. It is important to highlight that the value $pr_{out} = 0.01$ was used for both $N = 200$ and $N = 400$, while the value $pr_{out} = 0.005$ was used only for $N = 400$, being these choices considered to compare the results maintaining the probability and the expected number of outliers constant when the sample size increases. For the robust estimator we have chosen $\delta = 1.345$ in the Huber function (Equation 11) as a compromise between robustness and efficiency. Additionally, we have set $b_{N,\psi} = b_N = \nu N^{-\alpha}$, where $\nu = 0.15$ and $\alpha = 0.45$, being b_N the 'resampling bandwidth' of $I_N(\lambda_j)$, $b_{N,\psi}$ the 'robust resampling bandwidth' of $I_{N,\psi}(\lambda_j)$, these quantities were used to obtain the sets of probabilities of choosing the periodogram ordinates in the bootstrap procedure. The choice of a SARMA$(1,0) \times (1,0)_{\mathcal{S}}$ process was due to the fact that one of the real data time series analyzed in the Section 5 follows a seasonal time series model. Another motivation to simulate a SARMA$(1,0) \times (1,0)_{\mathcal{S}}$ process is the fact that all the theory given in Section 3.1 for an ARMA process is also valid for a SARMA process.

As a means to evaluate if the bootstrap estimates were able to mimic some features of the distributions of interest, we have calculated the estimates for the mean values $\overline{x} = \mathsf{E}(x)$, the standard deviation $\mathsf{SD}(x) = \sqrt{\mathsf{Var}(x)}$, the asymmetry coefficient $\gamma_1(x) = \mathsf{E}([\{x - \overline{x}\}/\mathsf{SD}(x)]^3)$, and the 95% confidence interval $\mathrm{CI}_{95\%}(y)$ together with its amplitude $\mathrm{A}(y)$ and coverage percentage $\mathrm{P}(y)$. The value of x is $\hat{\phi}^*$ for the AR(1) model and can be $\hat{\phi}^*$ or $\hat{\Phi}^*$ for the SARMA$(1,0) \times (1,0)_{\mathcal{S}}$ model, while y has the value $\overline{\hat{\phi}^*}$ for the AR(1) model and can be $\overline{\hat{\phi}}^*$ or $\overline{\hat{\Phi}}^*$ for the SARMA$(1,0) \times (1,0)_{\mathcal{S}}$ model. The results of the bootstrap estimates for the parameters are shown in Tables 1-9, for the AR(1) series, and in Tables 10-18 for the SARMA$(1,0) \times (1,0)_{\mathcal{S}}$ series. In the following, if a table has the column I_N or I_N^* it is to show the type of periodogram used: C denotes the classical and M designates the robust. For both models, the Bartlett-Priestley kernel was used to calculate the set of probabilities of the bootstrap. The bootstrap estimates were obtained thorough the generation of $REP_{MC} = 1000$ Monte Carlo replicates of $\{Z_t\}$ and, for each of them, $B = 5000$ bootstrap replicates of the periodogram were generated, with their related estimated parameters being denoted by $\hat{\phi}^{*(1)}, \hat{\phi}^{*(2)}, \ldots, \hat{\phi}^{*(B)}$ or by $\hat{\Phi}^{*(1)}, \hat{\Phi}^{*(2)}, \ldots, \hat{\Phi}^{*(B)}$, these quantities were used to estimate the aforementioned characteristics of the distributions of interest.

It is important to highlight that to avoid taking average of confidence intervals in the bootstrap procedure, which would be necessary due to the fact that each Monte Carlo replicate generates a confidence interval $\mathrm{CI}_{95\%}(x)$, where x takes the values of $\hat{\phi}^*$ or $\hat{\Phi}^*$, it was preferred to estimate the bootstrap confidence interval through the quantiles of the empirical distribution of the mean values $\overline{\hat{\phi}^*} = \sum_{i=1}^{B} \hat{\phi}^{*(i)}/B$ or $\overline{\hat{\Phi}^*} = \sum_{i=1}^{B} \hat{\Phi}^{*(i)}/B$. For each Monte Carlo replicate these intervals were denoted by $\mathrm{CI}_{95\%}(\overline{\hat{\phi}^*})$ with amplitude $\mathrm{A}(\overline{\hat{\phi}^*})$ and coverage percentage $\mathrm{P}(\overline{\hat{\phi}^*})$, or by $\mathrm{CI}_{95\%}(\overline{\hat{\Phi}^*})$ with amplitude $\mathrm{A}(\overline{\hat{\Phi}^*})$ and coverage percentage $\mathrm{P}(\overline{\hat{\Phi}^*})$. The choice of this methodology to estimate the bootstrap confidence interval is due to the fact that the average of intervals of certain confidence level usually does not maintain the same confidence level of the intervals of which the average is taken. In this context, we have to emphasize that Tables 1-18, which display the results of the bootstrap estimates, have the average values for all the calculated estimates (that in the case of the confidence interval as well as of its amplitude and coverage percentage were calculated based on a single value), and between parentheses are the standard deviations only of the estimates of the mean values, of the standard deviations, and of the asymmetries of the parameters. For the bootstrap confidence intervals, the coverage percentage $\mathrm{P}(x)$ was calculated as the percentage of times in which the true value of the bootstrap estimates, calculated for the uncontaminated series $\{Y_t\}$ (that can be the component referring to x of $\tilde{\boldsymbol{\varphi}}_W$

or $\tilde{\boldsymbol{\varphi}}_{W,\psi}$), is contained in the confidence interval of the bootstrap procedure $\mathrm{CI}_{95\%}(x)$ where x takes the values of $\overline{\hat{\phi}^*}$ or $\overline{\hat{\Phi}^*}$.

Tables 1-18 show that the bootstrap estimates for both the classical and the robust methodology have coverage percentages close to 95% in the scenarios without contamination, which demonstrates the efficient of both methodologies in this scenario. However, when there is data contamination by additive outliers, only the robust methodologies are able to maintain coverage percentages close to 95%, while the classical methodologies perform worse and worse when compared to the robust ones as the value of pr_{out} or of ω increases. In this context, it is important to emphasize that the confidence intervals of the robust approaches had coverage percentages tending to 95% as the sample size increases while the expected number of outliers is kept constant, i.e., when we go from the scenario with $N = 200$ and $pr_{out} = 0.01$ to the one with $N = 400$ and $pr_{out} = 0.005$, as in this case the outlier effect is diluted with the increase of N. Moreover, it should be noted that for the scenarios with contamination, the robust methodologies generated confidence intervals that, when compared to the classical methodologies, in addition to presenting coverage percentages closer to 95%, they also presented lower amplitudes. This gives empirical evidence that the robust local bootstrap is a good alternative to estimate confidence intervals of parameters of weakly stationary time series for which there is suspect of contamination by additive outliers. When compared to the local bootstrap of Paparoditis and Politis (1999), it has similar performance when there is no outlier contamination and it generates intervals with better performance in terms of both amplitude and coverage percentage in the presence of additive outliers in the data.

Table 1: Bootstrap Estimates for $\phi = 0.2$ with $REP_{MC} = 1000$, $B = 5000$, $pr_{out} = 0.01$ and $N = 200$.

ω	I_N^*	$\overline{\overline{\hat{\phi}^*}}$	$\mathsf{SD}(\hat{\phi}^*)$	$\gamma_1(\hat{\phi}^*)$	$\mathrm{CI}_{95\%}(\overline{\hat{\phi}^*})$	$\mathrm{A}(\overline{\hat{\phi}^*})$	$\mathrm{P}(\overline{\hat{\phi}^*})$
0	C	0.1816(0.0709)	0.0533(0.0076)	-0.1001(0.0743)	(0.0471,0.3160)	0.2689	0.9490
	M	0.1716(0.0713)	0.0534(0.0077)	-0.0964(0.0750)	(0.0350,0.3103)	0.2753	0.9470
4	C	0.1566(0.0724)	0.0544(0.0079)	-0.0897(0.0737)	(0.0123,0.2955)	0.2832	0.9390
	M	0.1652(0.0694)	0.0541(0.0077)	-0.0902(0.0715)	(0.0266,0.2926)	0.2660	0.9430
7	C	0.1282(0.0792)	0.0535(0.0073)	-0.0766(0.0751)	(-0.0157,0.2843)	0.3000	0.9140
	M	0.1662(0.0732)	0.0540(0.0076)	-0.0933(0.0730)	(0.0153,0.3074)	0.2921	0.9420

Table 2: Bootstrap Estimates for $\phi = 0.2$ with $REP_{MC} = 1000$, $B = 5000$, $pr_{out} = 0.005$ and $N = 400$.

ω	I_N^*	$\overline{\overline{\hat{\phi}^*}}$	$\mathsf{SD}(\hat{\phi}^*)$	$\gamma_1(\hat{\phi}^*)$	$\mathrm{CI}_{95\%}(\overline{\hat{\phi}^*})$	$\mathrm{A}(\overline{\hat{\phi}^*})$	$\mathrm{P}(\overline{\hat{\phi}^*})$
0	C	0.1929(0.0490)	0.0400(0.0043)	-0.0749(0.0481)	(0.0976,0.2910)	0.1934	0.9480
	M	0.1837(0.0496)	0.0401(0.0043)	-0.0716(0.0498)	(0.0844,0.2827)	0.1983	0.9490
4	C	0.1808(0.0489)	0.0401(0.0041)	-0.0673(0.0482)	(0.0852,0.2776)	0.1924	0.9400
	M	0.1814(0.0490)	0.0400(0.0041)	-0.0673(0.0471)	(0.0851,0.2740)	0.1889	0.9460
7	C	0.1540(0.0543)	0.0402(0.0041)	-0.0615(0.0480)	(0.0448,0.2587)	0.2139	0.9290
	M	0.1757(0.0485)	0.0401(0.0044)	-0.0665(0.0468)	(0.0765,0.2712)	0.1947	0.9450

Table 3: Bootstrap Estimates for $\phi = 0.2$ with $REP_{MC} = 1000$, $B = 5000$, $pr_{out} = 0.01$ and $N = 400$.

ω	I_N^*	$\overline{\overline{\hat{\phi}^*}}$	$\mathsf{SD}(\hat{\phi}^*)$	$\gamma_1(\hat{\phi}^*)$	$\mathrm{CI}_{95\%}(\overline{\hat{\phi}^*})$	$\mathrm{A}(\overline{\hat{\phi}^*})$	$\mathrm{P}(\overline{\hat{\phi}^*})$
4	C	0.1638(0.0497)	0.0402(0.0042)	-0.0641(0.0478)	(0.0665,0.2581)	0.1916	0.9120
	M	0.1737(0.0487)	0.0401(0.0042)	-0.0675(0.0492)	(0.0825,0.2694)	0.1869	0.9450
7	C	0.1325(0.0550)	0.0402(0.0040)	-0.0535(0.0492)	(0.0243,0.2400)	0.2157	0.8220
	M	0.1761(0.0501)	0.0401(0.0041)	-0.0685(0.0483)	(0.0772,0.2696)	0.1924	0.9400

Table 4: Bootstrap Estimates for $\phi = 0.5$ with $REP_{MC} = 1000$, $B = 5000$, $pr_{out} = 0.01$ and $N = 200$.

ω	I_N^*	$\overline{\overline{\hat{\phi}^*}}$	$\mathsf{SD}(\hat{\phi}^*)$	$\gamma_1(\hat{\phi}^*)$	$\mathrm{CI}_{95\%}(\overline{\hat{\phi}^*})$	$\mathrm{A}(\overline{\hat{\phi}^*})$	$\mathrm{P}(\overline{\hat{\phi}^*})$
0	C	0.4745(0.0631)	0.0481(0.0091)	-0.2818(0.0989)	(0.3438,0.5873)	0.2435	0.9430
	M	0.4546(0.0667)	0.0488(0.0090)	-0.2690(0.0976)	(0.3170,0.5756)	0.2586	0.9470
4	C	0.4184(0.0748)	0.0515(0.0090)	-0.2548(0.0987)	(0.2660,0.5645)	0.2985	0.9140
	M	0.4354(0.0685)	0.0506(0.0088)	-0.2651(0.1028)	(0.2934,0.5700)	0.2766	0.9380
7	C	0.3568(0.0980)	0.0526(0.0092)	-0.2181(0.0993)	(0.1688,0.5425)	0.3737	0.8100
	M	0.4412(0.0681)	0.0499(0.0090)	-0.2616(0.0984)	(0.2996,0.5647)	0.2651	0.9360

5 An Application to the Air Quality Area

The application is based on a data set (air pollutant variables) collected at Automatic Air Quality Monitoring Network (RAMQAr) in the Greater Vitória

Table 5: Bootstrap Estimates for $\phi = 0.5$ with $REP_{MC} = 1000$, $B = 5000$, $pr_{out} = 0.005$ and $N = 400$.

ω	I_N^*	$\overline{\hat{\phi}^*}$	$\mathsf{SD}(\hat{\phi}^*)$	$\gamma_1(\hat{\phi}^*)$	$\text{CI}_{95\%}(\overline{\hat{\phi}^*})$	$\text{A}(\overline{\hat{\phi}^*})$	$\text{P}(\overline{\hat{\phi}^*})$
0	C	0.4889(0.0438)	0.0356(0.0048)	-0.2078(0.0635)	(0.4012,0.5747)	0.1735	0.9460
	M	0.4689(0.0461)	0.0363(0.0049)	-0.1988(0.0606)	(0.3732,0.5593)	0.1861	0.9460
4	C	0.4597(0.0482)	0.0367(0.0049)	-0.1989(0.0613)	(0.3567,0.5509)	0.1942	0.9210
	M	0.4587(0.0448)	0.0368(0.0049)	-0.1962(0.0598)	(0.3708,0.5429)	0.1721	0.9430
7	C	0.4169(0.0644)	0.0381(0.0053)	-0.1788(0.0606)	(0.2917,0.5369)	0.2452	0.8610
	M	0.4590(0.0457)	0.0367(0.0049)	-0.1935(0.0602)	(0.3690,0.5461)	0.1771	0.9420

Table 6: Bootstrap Estimates for $\phi = 0.5$ with $REP_{MC} = 1000$, $B = 5000$, $pr_{out} = 0.01$ and $N = 400$.

ω	I_N^*	$\overline{\hat{\phi}^*}$	$\mathsf{SD}(\hat{\phi}^*)$	$\gamma_1(\hat{\phi}^*)$	$\text{CI}_{95\%}(\overline{\hat{\phi}^*})$	$\text{A}(\overline{\hat{\phi}^*})$	$\text{P}(\overline{\hat{\phi}^*})$
4	C	0.4347(0.0499)	0.0374(0.0047)	-0.1882(0.0595)	(0.3328,0.5251)	0.1923	0.7890
	M	0.4497(0.0465)	0.0369(0.0046)	-0.1934(0.0596)	(0.3568,0.5408)	0.1840	0.9380
7	C	0.3580(0.0661)	0.0396(0.0050)	-0.1518(0.0589)	(0.2284,0.4792)	0.2508	0.3910
	M	0.4497(0.0456)	0.0371(0.0049)	-0.1924(0.0578)	(0.3595,0.5370)	0.1775	0.9300

Table 7: Bootstrap Estimates for $\phi = 0.8$ with $REP_{MC} = 1000$, $B = 5000$, $pr_{out} = 0.01$ and $N = 200$.

ω	I_N^*	$\overline{\hat{\phi}^*}$	$\mathsf{SD}(\hat{\phi}^*)$	$\gamma_1(\hat{\phi}^*)$	$\text{CI}_{95\%}(\overline{\hat{\phi}^*})$	$\text{A}(\overline{\hat{\phi}^*})$	$\text{P}(\overline{\hat{\phi}^*})$
0	C	0.7677(0.0435)	0.0360(0.0102)	-0.6529(0.2035)	(0.6731,0.8410)	0.1679	0.9330
	M	0.7494(0.0479)	0.0377(0.0105)	-0.6260(0.1950)	(0.6410,0.8311)	0.1901	0.9400
4	C	0.7216(0.0622)	0.0420(0.0118)	-0.6117(0.2024)	(0.5812,0.8246)	0.2434	0.8470
	M	0.7259(0.0575)	0.0408(0.0114)	-0.6037(0.1934)	(0.5985,0.8275)	0.2290	0.9260
7	C	0.6509(0.0944)	0.0480(0.0144)	-0.5452(0.1932)	(0.4562,0.8127)	0.3565	0.7610
	M	0.7236(0.0569)	0.0406(0.0115)	-0.6007(0.1968)	(0.6020,0.8261)	0.2241	0.9100

Table 8: Bootstrap Estimates for $\phi = 0.8$ with $REP_{MC} = 1000$, $B = 5000$, $pr_{out} = 0.005$ and $N = 400$.

ω	I_N^*	$\overline{\hat{\phi}^*}$	$\mathsf{SD}(\hat{\phi}^*)$	$\gamma_1(\hat{\phi}^*)$	$\text{CI}_{95\%}(\overline{\hat{\phi}^*})$	$\text{A}(\overline{\hat{\phi}^*})$	$\text{P}(\overline{\hat{\phi}^*})$
0	C	0.7822(0.0324)	0.0257(0.0058)	-0.4800(0.1221)	(0.7154,0.8388)	0.1234	0.9430
	M	0.7664(0.0358)	0.0269(0.0060)	-0.4590(0.1165)	(0.6925,0.8298)	0.1373	0.9410
4	C	0.7624(0.0374)	0.0274(0.0062)	-0.4627(0.1220)	(0.6818,0.8284)	0.1466	0.9110
	M	0.7559(0.0368)	0.0276(0.0059)	-0.4498(0.1207)	(0.6793,0.8250)	0.1457	0.9350
7	C	0.7190(0.0584)	0.0316(0.0076)	-0.4377(0.1168)	(0.5982,0.8176)	0.2194	0.8160
	M	0.7515(0.0370)	0.0284(0.0063)	-0.4490(0.1138)	(0.6768,0.8206)	0.1438	0.9320

Region (GVR) in the Brazilian state of Espírito Santo, which is composed by nine monitoring stations placed in strategic locations and accounts for the measuring of several atmospheric pollutants and meteorological variables in

Table 9: Bootstrap Estimates for $\phi = 0.8$ with $REP_{MC} = 1000$, $B = 5000$, $pr_{out} = 0.01$ and $N = 400$.

ω	I_N^*	$\overline{\hat{\phi}^*}$	$\mathsf{SD}(\hat{\phi}^*)$	$\gamma_1(\hat{\phi}^*)$	$\mathrm{CI}_{95\%}(\overline{\hat{\phi}^*})$	$\mathrm{A}(\overline{\hat{\phi}^*})$	$\mathrm{P}(\overline{\hat{\phi}^*})$
4	C	0.7372(0.0439)	0.0303(0.0071)	-0.4451(0.1184)	(0.6446,0.8134)	0.1688	0.7790
	M	0.7410(0.0393)	0.0296(0.0068)	-0.4437(0.1187)	(0.6588,0.8131)	0.1543	0.9020
7	C	0.6658(0.0677)	0.0356(0.0079)	-0.3945(0.1150)	(0.5231,0.7824)	0.2593	0.3940
	M	0.7379(0.0401)	0.0295(0.0063)	-0.4320(0.1134)	(0.6500,0.8113)	0.1613	0.8720

the area. GVR is comprised of seven cities with a population of approximately 2 million inhabitants in an area of 2319 km^2. The region is situated along the South Atlantic coast of Brazil (latitude 20°19′15″S, longitude 40°20′10″W) and has a tropical humid climate, with average temperatures ranging from 24 °C to 30 °C. The data sets considered in this paper are of the pollutant Particulate Matter with diameter smaller than 10 µm (PM_{10}), measured hourly, in µg/m^3, collected at the stations located in Downtown Vila Velha and Jardim Camburi areas.

We will denote the PM_{10} concentrations in the stations of Downtown Vila Velha and Jardim Camburi by PM_{10}^{VV} and PM_{10}^{JC}, respectively. These data sets include daily average concentrations from January 1, 2018 to September 22, 2019, which keep a sample size, $N = 630$, multiple of the natural choice to the seasonality $\mathcal{S} = 7$ and it is equivalent to 90 full weeks. Due to skewness and some evidences of time varying variance, the natural logarithm transformation (log) was used and the plots of the $\log(PM_{10}^{VV})$ and $\log(PM_{10}^{JC})$ are displayed in Figures 1 and 2, respectively. From these figures, one can see large peaks of PM_{10} concentration which may be viewed here as outliers and, these high levels can provoke serious damage to some statistics, such as the mean and the standard deviation and, therefore, may affect the sample correlation structure as well as the periodogram of the series, causing misleading results. The existence of any outlier's effect and the presence of deterministic trends must be firstly removed from $\log(PM_{10}^{VV})$ and $\log(PM_{10}^{JC})$ before further analysis. This

Table 10: Bootstrap Estimates for $\phi = 0.5$, $\Phi = 0.2$, $s = 4$, $REP_{MC} = 1000$, $B = 5000$, $pr_{out} = 0.01$ and $N = 200$.

ω	I_N^*	$\overline{\hat{\phi}^*}$	$\overline{\hat{\Phi}^*}$	SD($\hat{\phi}^*$)	SD($\hat{\Phi}^*$)	$\gamma_1(\hat{\phi}^*)$	$\gamma_1(\hat{\Phi}^*)$	$\mathrm{CI}_{95\%}(\overline{\hat{\phi}^*})$	$\mathrm{CI}_{95\%}(\overline{\hat{\Phi}^*})$	A($\overline{\hat{\phi}^*}$)	A($\overline{\hat{\Phi}^*}$)	P($\overline{\hat{\phi}^*}$)	P($\overline{\hat{\Phi}^*}$)
0	C	0.4761(0.0662)	0.1875(0.0675)	0.0494(0.0088)	0.0541(0.0081)	-0.2711(0.1035)	-0.1121(0.0818)	(0.3402,0.5958)	(0.0556,0.3094)	0.2556	0.2538	0.9430	0.9450
	M	0.4565(0.0689)	0.1758(0.0669)	0.0503(0.0088)	0.0542(0.0081)	-0.2588(0.1028)	-0.1028(0.0807)	(0.3214,0.5855)	(0.0415,0.3037)	0.2641	0.2622	0.9480	0.9490
4	C	0.4241(0.0705)	0.1658(0.0695)	0.0517(0.0091)	0.0544(0.0080)	-0.2391(0.1063)	-0.0994(0.0804)	(0.2867,0.5582)	(0.0229,0.2994)	0.2715	0.2765	0.8860	0.9340
	M	0.4377(0.0650)	0.1699(0.0700)	0.0510(0.0089)	0.0544(0.0081)	-0.2460(0.1004)	-0.1014(0.0792)	(0.3079,0.5638)	(0.0360,0.3037)	0.2559	0.2677	0.9340	0.9440
7	C	0.3533(0.0946)	0.1389(0.0754)	0.0540(0.0089)	0.0539(0.0073)	-0.2011(0.0956)	-0.0847(0.0811)	(0.1709,0.5378)	(-0.0097,0.2826)	0.3669	0.2923	0.8100	0.8860
	M	0.4378(0.0662)	0.1698(0.0733)	0.0512(0.0090)	0.0546(0.0080)	-0.2470(0.0998)	-0.0983(0.0796)	(0.3057,0.5589)	(0.0201,0.3024)	0.2532	0.2823	0.9320	0.9400

Table 11: Bootstrap Estimates for $\phi = 0.5$, $\Phi = 0.2$, $s = 4$, $REP_{MC} = 1000$, $B = 5000$, $pr_{out} = 0.005$ and $N = 400$.

ω	I_N^*	$\overline{\hat{\phi}^*}$	$\overline{\hat{\Phi}^*}$	SD($\hat{\phi}^*$)	SD($\hat{\Phi}^*$)	$\gamma_1(\hat{\phi}^*)$	$\gamma_1(\hat{\Phi}^*)$	$\mathrm{CI}_{95\%}(\overline{\hat{\phi}^*})$	$\mathrm{CI}_{95\%}(\overline{\hat{\Phi}^*})$	A($\overline{\hat{\phi}^*}$)	A($\overline{\hat{\Phi}^*}$)	P($\overline{\hat{\phi}^*}$)	P($\overline{\hat{\Phi}^*}$)
0	C	0.4855(0.0451)	0.1940(0.0497)	0.0360(0.0047)	0.0403(0.0044)	-0.1898(0.0613)	-0.0773(0.0510)	(0.3942,0.5680)	(0.0980,0.2891)	0.1738	0.1911	0.9440	0.9470
	M	0.4653(0.0468)	0.1829(0.0501)	0.0369(0.0048)	0.0403(0.0043)	-0.1816(0.0609)	-0.0737(0.0521)	(0.3666,0.5556)	(0.0838,0.2790)	0.1890	0.1952	0.9500	0.9500
4	C	0.4602(0.0480)	0.1788(0.0490)	0.0372(0.0047)	0.0403(0.0041)	-0.1788(0.0599)	-0.0727(0.0494)	(0.3638,0.5490)	(0.0807,0.2734)	0.1852	0.1927	0.9060	0.9460
	M	0.4594(0.0466)	0.1765(0.0489)	0.0371(0.0047)	0.0404(0.0042)	-0.1764(0.0588)	-0.0718(0.0480)	(0.3667,0.5467)	(0.0801,0.2681)	0.1800	0.1880	0.9460	0.9490
7	C	0.4176(0.0624)	0.1599(0.0523)	0.0386(0.0049)	0.0400(0.0043)	-0.1629(0.0614)	-0.0660(0.0494)	(0.2964,0.5334)	(0.0564,0.2605)	0.2370	0.2041	0.8150	0.9100
	M	0.4606(0.0459)	0.1773(0.0487)	0.0371(0.0045)	0.0402(0.0042)	-0.1788(0.0616)	-0.0727(0.0498)	(0.3693,0.5442)	(0.0790,0.2698)	0.1749	0.1908	0.9410	0.9460

Table 12: Bootstrap Estimates for $\phi = 0.5$, $\Phi = 0.2$, $s = 4$, $REP_{MC} = 1000$, $B = 5000$, $pr_{out} = 0.01$ and $N = 400$.

ω	I_N^*	$\overline{\hat{\phi}^*}$	$\overline{\hat{\Phi}^*}$	SD($\hat{\phi}^*$)	SD($\hat{\Phi}^*$)	$\gamma_1(\hat{\phi}^*)$	$\gamma_1(\hat{\Phi}^*)$	$\mathrm{CI}_{95\%}(\overline{\hat{\phi}^*})$	$\mathrm{CI}_{95\%}(\overline{\hat{\Phi}^*})$	A($\overline{\hat{\phi}^*}$)	A($\overline{\hat{\Phi}^*}$)	P($\overline{\hat{\phi}^*}$)	P($\overline{\hat{\Phi}^*}$)
4	C	0.4375(0.0527)	0.1683(0.0513)	0.0383(0.0048)	0.0404(0.0041)	-0.1725(0.0601)	-0.0686(0.0499)	(0.3261,0.5393)	(0.0638,0.2727)	0.2132	0.2089	0.8510	0.9240
	M	0.4528(0.0479)	0.1750(0.0505)	0.0375(0.0047)	0.0402(0.0041)	-0.1760(0.0602)	-0.0705(0.0516)	(0.3574,0.5473)	(0.0815,0.2779)	0.1899	0.1964	0.9300	0.9410
7	C	0.3642(0.0686)	0.1392(0.0541)	0.0404(0.0052)	0.0401(0.0040)	-0.1442(0.0619)	-0.0580(0.0506)	(0.2218,0.4905)	(0.0312,0.2433)	0.2687	0.2121	0.4840	0.8380
	M	0.4502(0.0487)	0.1718(0.0521)	0.0377(0.0046)	0.0402(0.0041)	-0.1738(0.0610)	-0.0690(0.0502)	(0.3512,0.5399)	(0.0701,0.2707)	0.1887	0.2006	0.9280	0.9400

Table 13: Bootstrap Estimates for $\phi = 0.5$, $\Phi = 0.5$, $s = 4$, $REP_{MC} = 1000$, $B = 5000$, $pr_{out} = 0.01$ and $N = 200$.

ω	I_N^*	$\overline{\hat{\phi}^*}$	$\overline{\hat{\Phi}^*}$	$\mathsf{SD}(\hat{\phi}^*)$	$\mathsf{SD}(\hat{\Phi}^*)$	$\gamma_1(\hat{\phi}^*)$	$\gamma_1(\hat{\Phi}^*)$	$\mathrm{CI}_{95\%}(\overline{\hat{\phi}^*})$	$\mathrm{CI}_{95\%}(\overline{\hat{\Phi}^*})$	$\mathrm{A}(\overline{\hat{\phi}^*})$	$\mathrm{A}(\overline{\hat{\Phi}^*})$	$\mathrm{P}(\overline{\hat{\phi}^*})$	$\mathrm{P}(\overline{\hat{\Phi}^*})$
0	C	0.4771(0.0655)	0.4731(0.0629)	0.0489(0.0086)	0.0484(0.0091)	-0.2654(0.1028)	-0.2901(0.1036)	(0.3421,0.5974)	(0.3306,0.5868)	0.2553	0.2562	0.9480	0.9460
	M	0.4502(0.0705)	0.4483(0.0662)	0.0504(0.0085)	0.0495(0.0090)	-0.2506(0.1006)	-0.2734(0.1016)	(0.3025,0.5803)	(0.3028,0.5675)	0.2778	0.2647	0.9510	0.9420
4	C	0.4223(0.0760)	0.4220(0.0726)	0.0535(0.0099)	0.0518(0.0094)	-0.2393(0.1060)	-0.2704(0.1057)	(0.2754,0.5649)	(0.2763,0.5616)	0.2895	0.2853	0.9070	0.8970
	M	0.4280(0.0711)	0.4282(0.0676)	0.0528(0.0098)	0.0512(0.0094)	-0.2397(0.1029)	-0.2689(0.1008)	(0.2876,0.5622)	(0.2800,0.5553)	0.2746	0.2753	0.9370	0.9300
7	C	0.3537(0.0945)	0.3508(0.0938)	0.0560(0.0101)	0.0538(0.0095)	-0.1990(0.1031)	-0.2296(0.1037)	(0.1639,0.5323)	(0.1646,0.5345)	0.3684	0.3699	0.7750	0.7930
	M	0.4295(0.0690)	0.4227(0.0705)	0.0529(0.0095)	0.0516(0.0094)	-0.2424(0.1059)	-0.2652(0.1029)	(0.2906,0.5578)	(0.2833,0.5540)	0.2672	0.2707	0.9250	0.9230

Table 14: Bootstrap Estimates for $\phi = 0.5$, $\Phi = 0.5$, $s = 4$, $REP_{MC} = 1000$, $B = 5000$, $pr_{out} = 0.005$ and $N = 400$.

ω	I_N^*	$\overline{\hat{\phi}^*}$	$\overline{\hat{\Phi}^*}$	$\mathsf{SD}(\hat{\phi}^*)$	$\mathsf{SD}(\hat{\Phi}^*)$	$\gamma_1(\hat{\phi}^*)$	$\gamma_1(\hat{\Phi}^*)$	$\mathrm{CI}_{95\%}(\overline{\hat{\phi}^*})$	$\mathrm{CI}_{95\%}(\overline{\hat{\Phi}^*})$	$\mathrm{A}(\overline{\hat{\phi}^*})$	$\mathrm{A}(\overline{\hat{\Phi}^*})$	$\mathrm{P}(\overline{\hat{\phi}^*})$	$\mathrm{P}(\overline{\hat{\Phi}^*})$
0	C	0.4871(0.0450)	0.4879(0.0436)	0.0359(0.0048)	0.0357(0.0048)	-0.1894(0.0636)	-0.2119(0.0635)	(0.3957,0.5724)	(0.4015,0.5671)	0.1767	0.1656	0.9490	0.9430
	M	0.4620(0.0475)	0.4626(0.0464)	0.0371(0.0048)	0.0366(0.0048)	-0.1785(0.0641)	-0.2024(0.0638)	(0.3686,0.5554)	(0.3677,0.5514)	0.1868	0.1837	0.9500	0.9500
4	C	0.4574(0.0496)	0.4565(0.0490)	0.0376(0.0048)	0.0370(0.0050)	-0.1787(0.0644)	-0.1970(0.0628)	(0.3540,0.5490)	(0.3518,0.5474)	0.1950	0.1956	0.9120	0.9030
	M	0.4503(0.0488)	0.4512(0.0476)	0.0378(0.0049)	0.0371(0.0050)	-0.1771(0.0633)	-0.1954(0.0626)	(0.3506,0.5446)	(0.3611,0.5435)	0.1940	0.1824	0.9430	0.9420
7	C	0.4138(0.0666)	0.4109(0.0645)	0.0393(0.0053)	0.0384(0.0052)	-0.1600(0.0647)	-0.1771(0.0634)	(0.2806,0.5393)	(0.2845,0.5329)	0.2587	0.2484	0.8360	0.8340
	M	0.4511(0.0492)	0.4493(0.0482)	0.0377(0.0048)	0.0370(0.0050)	-0.1768(0.0626)	-0.1933(0.0635)	(0.3541,0.5440)	(0.3537,0.5403)	0.1899	0.1866	0.9380	0.9360

Table 15: Bootstrap Estimates for $\phi = 0.5$, $\Phi = 0.5$, $s = 4$, $REP_{MC} = 1000$, $B = 5000$, $pr_{out} = 0.01$ and $N = 400$.

ω	I_N^*	$\overline{\hat{\phi}^*}$	$\overline{\hat{\Phi}^*}$	$\mathsf{SD}(\hat{\phi}^*)$	$\mathsf{SD}(\hat{\Phi}^*)$	$\gamma_1(\hat{\phi}^*)$	$\gamma_1(\hat{\Phi}^*)$	$\mathrm{CI}_{95\%}(\overline{\hat{\phi}^*})$	$\mathrm{CI}_{95\%}(\overline{\hat{\Phi}^*})$	$\mathrm{A}(\overline{\hat{\phi}^*})$	$\mathrm{A}(\overline{\hat{\Phi}^*})$	$\mathrm{P}(\overline{\hat{\phi}^*})$	$\mathrm{P}(\overline{\hat{\Phi}^*})$
4	C	0.4328(0.0527)	0.4293(0.0522)	0.0388(0.0051)	0.0379(0.0050)	-0.1688(0.0637)	-0.1877(0.0620)	(0.3285,0.5382)	(0.3281,0.5275)	0.2097	0.1994	0.8650	0.8320
	M	0.4398(0.0497)	0.4366(0.0480)	0.0383(0.0051)	0.0375(0.0048)	-0.1714(0.0631)	-0.1870(0.0616)	(0.3385,0.5367)	(0.3385,0.5280)	0.1982	0.1895	0.9350	0.9380
7	C	0.3645(0.0683)	0.3642(0.0668)	0.0418(0.0055)	0.0401(0.0051)	-0.1390(0.0634)	-0.1551(0.0623)	(0.2391,0.4954)	(0.2380,0.4930)	0.2563	0.2550	0.5070	0.4990
	M	0.4406(0.0505)	0.4396(0.0477)	0.0389(0.0052)	0.0378(0.0048)	-0.1703(0.0611)	-0.1897(0.0599)	(0.3364,0.5376)	(0.3400,0.5305)	0.2012	0.1905	0.9220	0.9230

Table 16: Bootstrap Estimates for $\phi = 0.5$, $\Phi = 0.7$, $s = 4$, $REP_{MC} = 1000$, $B = 5000$, $pr_{out} = 0.01$ and $N = 200$.

ω	I_N^*	$\overline{\hat{\phi}^*}$	$\overline{\hat{\Phi}^*}$	$\mathsf{SD}(\hat{\phi}^*)$	$\mathsf{SD}(\hat{\Phi}^*)$	$\gamma_1(\hat{\phi}^*)$	$\gamma_1(\hat{\Phi}^*)$	$\mathrm{CI}_{95\%}(\overline{\hat{\phi}^*})$	$\mathrm{CI}_{95\%}(\overline{\hat{\Phi}^*})$	$\mathrm{A}(\overline{\hat{\phi}^*})$	$\mathrm{A}(\overline{\hat{\Phi}^*})$	$\mathrm{P}(\overline{\hat{\phi}^*})$	$\mathrm{P}(\overline{\hat{\Phi}^*})$
0	C	0.4784(0.0667)	0.6616(0.0533)	0.0509(0.0093)	0.0430(0.0105)	-0.2591(0.1061)	-0.4998(0.1588)	(0.3436,0.6033)	(0.5505,0.7587)	0.2597	0.2082	0.9490	0.9430
	M	0.4453(0.0737)	0.6358(0.0579)	0.0524(0.0093)	0.0443(0.0104)	-0.2418(0.1042)	-0.4694(0.1503)	(0.2966,0.5848)	(0.5084,0.7429)	0.2882	0.2345	0.9460	0.9490
4	C	0.4160(0.0791)	0.6050(0.0706)	0.0544(0.0094)	0.0471(0.0108)	-0.2285(0.1053)	-0.4484(0.1457)	(0.2584,0.5642)	(0.4563,0.7309)	0.3058	0.2746	0.9060	0.8720
	M	0.4140(0.0750)	0.6046(0.0667)	0.0540(0.0090)	0.0465(0.0102)	-0.2249(0.1005)	-0.4353(0.1432)	(0.2604,0.5614)	(0.4600,0.7227)	0.3010	0.2627	0.9350	0.9160
7	C	0.3447(0.0965)	0.5296(0.0975)	0.0573(0.0107)	0.0522(0.0120)	-0.1804(0.1109)	-0.3982(0.1527)	(0.1648,0.5414)	(0.3313,0.7179)	0.3766	0.3866	0.8170	0.8100
	M	0.4063(0.0750)	0.6024(0.0654)	0.0548(0.0099)	0.0469(0.0111)	-0.2192(0.1011)	-0.4392(0.1421)	(0.2547,0.5481)	(0.4735,0.7200)	0.2934	0.2465	0.9190	0.9100

Table 17: Bootstrap Estimates for $\phi = 0.5$, $\Phi = 0.7$, $s = 4$, $REP_{MC} = 1000$, $B = 5000$, $pr_{out} = 0.005$ and $N = 400$.

ω	I_N^*	$\overline{\hat{\phi}^*}$	$\overline{\hat{\Phi}^*}$	$\mathsf{SD}(\hat{\phi}^*)$	$\mathsf{SD}(\hat{\Phi}^*)$	$\gamma_1(\hat{\phi}^*)$	$\gamma_1(\hat{\Phi}^*)$	$\mathrm{CI}_{95\%}(\overline{\hat{\phi}^*})$	$\mathrm{CI}_{95\%}(\overline{\hat{\Phi}^*})$	$\mathrm{A}(\overline{\hat{\phi}^*})$	$\mathrm{A}(\overline{\hat{\Phi}^*})$	$\mathrm{P}(\overline{\hat{\phi}^*})$	$\mathrm{P}(\overline{\hat{\Phi}^*})$
0	C	0.4887(0.0449)	0.6811(0.0390)	0.0360(0.0047)	0.0301(0.0054)	-0.1979(0.0607)	-0.3506(0.0888)	(0.3946,0.5706)	(0.5974,0.7486)	0.1760	0.1512	0.9500	0.9440
	M	0.4560(0.0494)	0.6568(0.0422)	0.0374(0.0047)	0.0313(0.0054)	-0.1809(0.0612)	-0.3326(0.0875)	(0.3560,0.5482)	(0.5644,0.7278)	0.1922	0.1634	0.9430	0.9450
4	C	0.4528(0.0530)	0.6513(0.0446)	0.0382(0.0053)	0.0322(0.0058)	-0.1780(0.0636)	-0.3354(0.0903)	(0.3440,0.5546)	(0.5566,0.7322)	0.2106	0.1756	0.9280	0.9110
	M	0.4394(0.0510)	0.6416(0.0439)	0.0387(0.0051)	0.0324(0.0059)	-0.1737(0.0615)	-0.3246(0.0861)	(0.3393,0.5374)	(0.5541,0.7274)	0.1981	0.1733	0.9410	0.9380
7	C	0.4055(0.0702)	0.6055(0.0641)	0.0399(0.0054)	0.0351(0.0066)	-0.1559(0.0705)	-0.3119(0.0917)	(0.2708,0.5386)	(0.4773,0.7214)	0.2678	0.2441	0.8320	0.8280
	M	0.4351(0.0540)	0.6394(0.0437)	0.0387(0.0050)	0.0326(0.0058)	-0.1714(0.0670)	-0.3256(0.0880)	(0.3331,0.5384)	(0.5497,0.7250)	0.2053	0.1753	0.9340	0.9330

Table 18: Bootstrap Estimates for $\phi = 0.5$, $\Phi = 0.7$, $s = 4$, $REP_{MC} = 1000$, $B = 5000$, $pr_{out} = 0.01$ and $N = 400$.

ω	I_N^*	$\overline{\hat{\phi}^*}$	$\overline{\hat{\Phi}^*}$	$\mathsf{SD}(\hat{\phi}^*)$	$\mathsf{SD}(\hat{\Phi}^*)$	$\gamma_1(\hat{\phi}^*)$	$\gamma_1(\hat{\Phi}^*)$	$\mathrm{CI}_{95\%}(\overline{\hat{\phi}^*})$	$\mathrm{CI}_{95\%}(\overline{\hat{\Phi}^*})$	$\mathrm{A}(\overline{\hat{\phi}^*})$	$\mathrm{A}(\overline{\hat{\Phi}^*})$	$\mathrm{P}(\overline{\hat{\phi}^*})$	$\mathrm{P}(\overline{\hat{\Phi}^*})$
4	C	0.4229(0.0566)	0.6248(0.0483)	0.0394(0.0050)	0.0342(0.0058)	-0.1673(0.0635)	-0.3214(0.0876)	(0.3159,0.5336)	(0.5264,0.7148)	0.2177	0.1884	0.8170	0.7820
	M	0.4201(0.0540)	0.6261(0.0445)	0.0392(0.0049)	0.0337(0.0057)	-0.1664(0.0625)	-0.3183(0.0876)	(0.3153,0.5280)	(0.5352,0.7105)	0.2127	0.1753	0.9150	0.9010
7	C	0.3457(0.0709)	0.5456(0.0670)	0.0423(0.0053)	0.0388(0.0071)	-0.1266(0.0690)	-0.2781(0.0876)	(0.2026,0.4907)	(0.4148,0.6808)	0.2881	0.2660	0.5100	0.4370
	M	0.4156(0.0558)	0.6225(0.0445)	0.0395(0.0050)	0.0340(0.0062)	-0.1651(0.0630)	-0.3169(0.0886)	(0.3019,0.5253)	(0.5349,0.7054)	0.2234	0.1705	0.9140	0.8840

will be discussed in the sequence, where a linear model with errors following an AR(p) process is fitted to $\log(\mathrm{PM}_{10}^{\mathrm{VV}})$ and a linear model with errors following a SARMA$(\tilde{p}, 0) \times (P, 0)_{\mathcal{S}}$ process is fitted to $\log(\mathrm{PM}_{10}^{\mathrm{JC}})$.

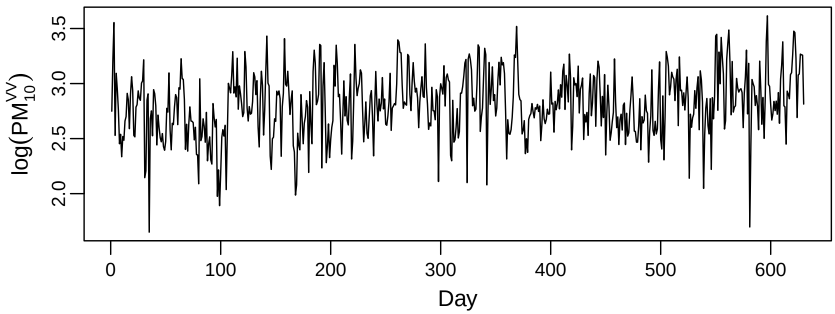

Figure 1: Plot of the $\log(\mathrm{PM}_{10}^{\mathrm{VV}})$ time series.

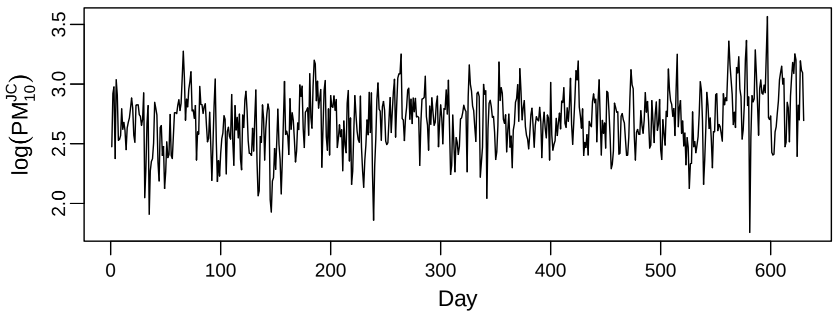

Figure 2: Plot of the $\log(\mathrm{PM}_{10}^{\mathrm{JC}})$ time series.

From the analysis of Figures 1 and 2, it can be concluded that both time series under study have a linear trend and a more complex trend that can be modeled by cubic b-splines basis functions $B_k^3(t)$ with $d_f = 8$ and $\tilde{d}_f = 7$ degrees of freedom, for the series $\log(\mathrm{PM}_{10}^{\mathrm{VV}})$ and $\log(\mathrm{PM}_{10}^{\mathrm{JC}})$, respectively. Hence, the following model is suggested here to fit the PM_{10} concentrations of

Downtown Vila Velha

$$\log(\mathrm{PM}_{10,t}^{\mathrm{VV}}) = \mu + \alpha t + \sum_{k=1}^{d_f} B_k^3(t)\beta_k + Y_t; \tag{23}$$

$$\phi_p(B)Y_t = \epsilon_t, \tag{24}$$

where B is the backshift operator that satisfies $B^j x_t = x_{t-j}$, additionally, we have that $\phi_p(B) = 1 - \phi_1 B - \phi_2 B^2 - \cdots - \phi_p B^p$. While for the Jardim Camburi data we propose the use of

$$\log(\mathrm{PM}_{10,t}^{\mathrm{JC}}) = \tilde{\mu} + \tilde{\alpha} t + \sum_{k=1}^{\tilde{d}_f} B_k^3(t)\tilde{\beta}_k + \tilde{Y}_t; \tag{25}$$

$$\Phi_P(B^{\mathcal{S}})\tilde{\phi}_{\tilde{p}}(B)\tilde{Y}_t = \tilde{\epsilon}_t, \tag{26}$$

where B is the backshift operator, $\tilde{\phi}_{\tilde{p}}(B) = 1 - \tilde{\phi}_1 B - \tilde{\phi}_2 B^2 - \cdots - \tilde{\phi}_{\tilde{p}} B^{\tilde{p}}$, $\Phi_P(B^{\mathcal{S}}) = 1 - \Phi_1 B^{\mathcal{S}} - \Phi_2 B^{2\mathcal{S}} - \cdots - \Phi_P B^{P\mathcal{S}}$, and the superscript $\tilde{}$ was used to differentiate the parameters of the linear model and of the time series related to Jardim Camburi from the ones regarding Downtown Vila Velha.

The model in Equations 23 and 24 as well as the one of Equations 25 and 26 were fitted based on following two steps procedure: (i) the linear models in (23) and (25) are estimated through the ordinary least squares procedure; and (ii) the AR(p) model in (24) and the SARMA($\tilde{p}$, 0) $\times$ (P, 0)$_{\mathcal{S}}$ model in (26) are fitted to the residuals of their respective linear model in step (i), where the AR with order p as well as the AR with order $\tilde{p}$, and the seasonal AR with order P, are identified through the Schwartz Information Criterion (BIC) proposed by Schwarz (1978).

The estimated coefficients of the linear models in Equations 23 and 25, fitted in the first step, are shown in Tables 19 and 20, respectively. The residuals of the linear models did not results in rejecting the null hypothesis of level stationarity of the KPSS test, with a p-value > 0.05. In order to appropriately select the model to fit these residuals, it is important to analyze their corresponding ACFs which are displayed in Figures 3 and 4, respectively. The ACF of Figure 3 shows that the residuals may follow an autoregressive model because it tails off as exponential decay, while the ACF of Figure 4 resembles the one of a seasonal model with $\mathcal{S} = 7$ because it has peaks of autocorrelation for lags multiple of seven. These are the reasons that motivated the choices of fitting an AR(p) model and a SARMA$(\tilde{p}, 0) \times (P, 0)_{\mathcal{S}}$ model in the second step.

Table 19: Estimated coefficients of the linear model for the $\log(\text{PM}_{10}^{\text{VV}})$ time series.

Parameter	μ	α	β_1	β_2	β_3	β_4	β_5	β_6	β_7	β_8
Estimate	2.9350	0.0003	-0.4426	-0.0755	-0.4514	-0.1064	-0.2772	0.0034	-0.1925	-0.1756

Table 20: Estimated coefficients of the linear model for the $\log(\text{PM}_{10}^{\text{JC}})$ time series.

Parameter	$\tilde{\mu}$	$\tilde{\alpha}$	$\tilde{\beta}_1$	$\tilde{\beta}_2$	$\tilde{\beta}_3$	$\tilde{\beta}_4$	$\tilde{\beta}_5$	$\tilde{\beta}_6$	$\tilde{\beta}_7$
Estimate	2.7880	0.0003	-0.3985	0.0454	-0.4135	-0.1085	-0.1351	-0.1177	-0.2572

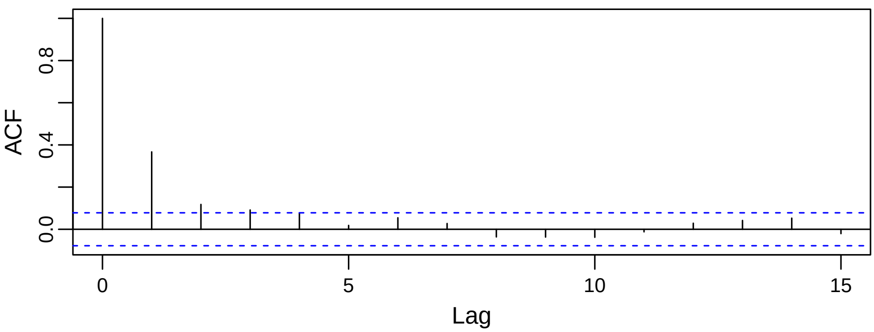

Figure 3: ACF of the residuals of the linear model for the $\log(\text{PM}_{10}^{\text{VV}})$ time series.

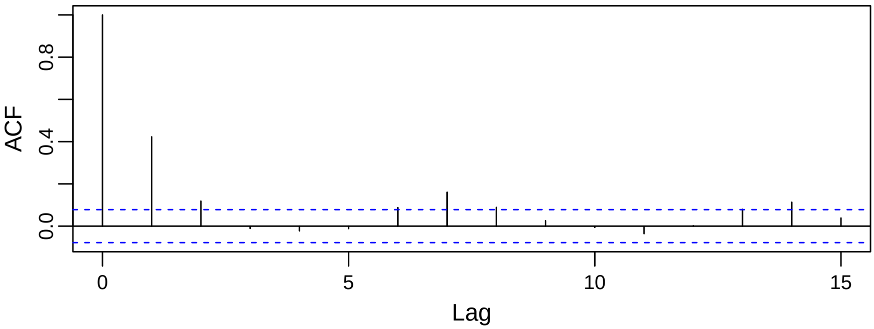

Figure 4: ACF of the residuals of the linear model for the $\log(\text{PM}_{10}^{\text{JC}})$ time series.

The BIC criterion was used to identify the orders of the models and the results are displayed in Tables 21 and 22. In order to keep consistency with the simulation study, $\delta = 1.345$ was fixed in the Huber function (Equation 11).

Table 21: Selected AR orders using the BIC for the $\log(\text{PM}_{10}^{\text{VV}})$ time series.

I_N	BIC	p
C	-1696.445	1
M	-1695.562	1

Table 22: Selected AR orders and seasonal AR orders using the BIC for the $\log(\text{PM}_{10}^{\text{JC}})$ time series.

I_N	BIC	$\tilde{p}$	P
C	-1935.253	1	1
M	-1934.989	1	1

The exact estimates of the AR(p) coefficients are displayed in Table 23 while the SARMA$(\tilde{p}, 0) \times (P, 0)_{\mathcal{S}}$ coefficients are shown in Table 24. Based on these results, it is clear that the robust methods always provided higher coefficient estimates. In this context, we have that for the AR(p) model the robust estimate of ϕ_1 was 10.4% bigger than its classical counterpart, while for the SARMA$(\tilde{p}, 0) \times (P, 0)_{\mathcal{S}}$ model we have that, for instance, the robust estimate of Φ_1 was 13.5% bigger than the classical one. This indicates that the high levels of the pollutant PM_{10} presented the effects of additive outliers in both the $\log(PM_{10}^{VV})$ and the $\log(PM_{10}^{JC})$ series since the classical estimates suffered from memory loss while their robust counterparts were resistant to outlier contamination.

Table 23: Exact estimates of the AR(p) coefficients for the $\log(PM_{10}^{VV})$ time series.

I_N	$\hat{\phi}_1$
C	0.3642
M	0.4021

Table 24: Exact estimates of the SARMA$(p, 0) \times (P, 0)_{\mathcal{S}}$ coefficients for the $\log(PM_{10}^{JC})$ time series.

I_N	$\hat{\tilde{\phi}}_1$	$\hat{\Phi}_1$
C	0.4181	0.1451
M	0.4203	0.1647

The classical ACF of the residuals of each estimated model is shown in Figure 5 for the $\log(PM_{10}^{VV})$ series, and in Figure 6 for the $\log(PM_{10}^{JC})$ series. It can be seen that for both series all the models were able to fully explain the correlation structure of the data, despite the eventual outliers effect. Based on the ACF of the residuals, the two estimation methods for both the AR(p) and the SARMA$(\tilde{p}, 0) \times (P, 0)_{\mathcal{S}}$ models are comparable since all the estimated residuals look like a white noise process.

The bootstrap estimates of the confidence intervals of the estimated coefficients for $B = 5000$ are given in Table 25 for the AR(p) coefficients, and in Table 26 for the SARMA$(\tilde{p}, 0) \times (P, 0)_{\mathcal{S}}$ coefficients. It is important to highlight that, similarly to the Monte Carlo experiment, we have chosen for both models $b_{N,\psi} = b_N = 0.15N^{-0.45}$ to obtain the set of probabilities to choose

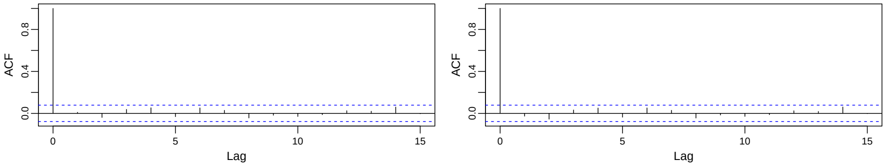

(a) C (b) M

Figure 5: ACF of the residuals of the AR(p) fit for the $\log(\mathrm{PM}_{10}^{\mathrm{VV}})$ time series.

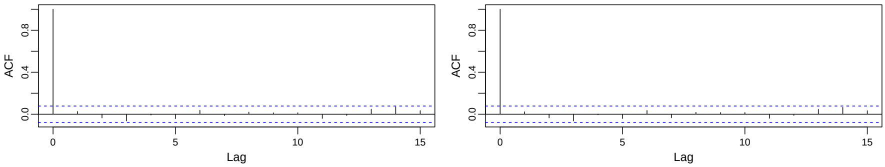

(a) C (b) M

Figure 6: ACF of the residuals of the $\mathrm{SARMA}(\tilde{p}, 0) \times (P, 0)_{\mathcal{S}}$ fit for the $\log(\mathrm{PM}_{10}^{\mathrm{JC}})$ time series.

the periodogram ordinates in the bootstrap procedure. Based on these results, it is possible to see that the confidence intervals of the classical method have a left shift in their lower limits when compared to the ones of its robust counterpart. This is also evidence that both the $\log(\mathrm{PM}_{10}^{\mathrm{VV}})$ and the $\log(\mathrm{PM}_{10}^{\mathrm{JC}})$ time series suffered from the effects of additive outliers contamination.

Table 25: Bootstrap estimates of the 95% confidence interval of the AR(p) coefficients for the $\log(\mathrm{PM}_{10}^{\mathrm{VV}})$ time series.

I_N^*	$\mathrm{CI}_{95\%}(\hat{\phi}_1^*)$
C	(0.3015, 0.4259)
M	(0.3402, 0.4635)

Table 26: Bootstrap estimates of the 95% confidence interval of the $\mathrm{SARMA}(\tilde{p}, 0) \times (P, 0)_{\mathcal{S}}$ coefficients for the $\log(\mathrm{PM}_{10}^{\mathrm{JC}})$ time series.

I_N^*	$\mathrm{CI}_{95\%}(\hat{\tilde{\phi}}_1^*)$	$\mathrm{CI}_{95\%}(\hat{\Phi}_1^*)$
C	(0.3505, 0.4692)	(0.0034, 0.2378)
M	(0.3520, 0.4720)	(0.0195, 0.2464)

6 Conclusions

The robust version of the local bootstrap in the periodogram, presented in this paper, had its finite sample performance compared to the one of the classical bootstrap, through a Monte Carlo experiment. This empirical investigation showed that both the robust and the classical versions of the bootstrap performed well when the time series did not have outliers. However, when there was contamination by additive outliers, the classical bootstrap had its performance completely affected, while the robust one proved to be very resistant to the contamination, maintaining the coverage percentages of the confidence intervals close to 95% and presenting lower amplitudes than the classical bootstrap. The daily mean concentrations of the PM_{10} collected in the stations of Downtown Vila Velha and Jardim Camburi, in the Brazilian state of Espírito Santo, were analyzed as an application of the methodologies studied in this paper. This analysis led to the conclusion that the memory loss occurred in the classical bootstrap caused it to generate confidence intervals dislocated to the left when compared to the ones obtained by the robust bootstrap. Based on these investigations, it is possible to conclude that the robust version of the local bootstrap in the periodogram proved to be an alternative for estimating confidence intervals of parameters of models of weakly stationary time series contaminated by additive outliers.

Acknowledgements

The results in this paper are part of the PhD thesis of the first author in the PPGEA-UFES under supervision of the second and third authors. The authors gratefully acknowledge partial financial support from FAPES/ES, CAPES/Brazil and CNPq/Brazil.

References

Brockwell PJ, Davis RA (1991) Time Series: Theory and Methods, 2nd edn. Springer New York, https://doi.org/10.1007/978-1-4419-0320-4

Efron B (1979) Bootstrap methods: another look at the jackknife. Ann Stat 7(1):1–26. https://doi.org/10.1214/aos/1176344552

Fajardo FA, Reisen VA, Lévy-Leduc C, et al (2018) M-periodogram for the analysis of long-range-dependent time series. Stat 52(3):665–683. https://doi.org/10.1080/02331888.2018.1427751

Franke J, Härdle W (1992) On bootstrapping kernel spectral estimates. Ann Stat 20(1):121–145. https://doi.org/10.1214/aos/1176348515

Huber PJ (1964) Robust estimation of a location parameter. Ann Math Stat 35(1):73–101. https://doi.org/10.1214/aoms/1177703732

Kreiss JP, Paparoditis E (2003) Autoregressive-aided periodogram bootstrap for time series. Ann Stat 31(6):1923–1955. https://doi.org/10.1214/aos/1074290332

Kreiss JP, Paparoditis E (2011) Bootstrap methods for dependent data: A review. J Korean Stat Soc 40(4):357–378. https://doi.org/10.1016/j.jkss.2011.08.009

Lahiri SN (2003) Resampling Methods for Dependent Data. Springer New York, https://doi.org/10.1007/978-1-4757-3803-2

Molinares FF, Reisen VA, Cribari-Neto F (2009) Robust estimation in long-memory processes under additive outliers. J Stat Plan Inference 139(8):2511–2525. https://doi.org/10.1016/j.jspi.2008.12.014

Paparoditis E, Politis DN (1999) The local bootstrap for periodogram statistics. J Time Ser Anal 20(2):193–222. https://doi.org/10.1111/1467-9892.00133

Priestley MB (1981) Spectral Analysis and Time Series. Academic Press

Reisen VA, Lévy-Leduc C, Taqqu MS (2017) An M-estimator for the long-memory parameter. J Stat Plan Inference 187:44–55. https://doi.org/10.1016/j.jspi.2017.02.008

Reisen VA, Lévy-Leduc C, Cotta HHA, et al (2019) An overview of robust spectral estimators. In: Applied Condition Monitoring, vol 16. Springer International Publishing, p 204–224, https://doi.org/10.1007/978-3-030-22529-2_12

Schwarz G (1978) Estimating the dimension of a model. Ann Stat 6(2):461–464. https://doi.org/10.1214/aos/1176344136

Singh K (1981) On the asymptotic accuracy of Efron's bootstrap. Ann Stat 9(6):1187–1195. https://doi.org/10.1214/aos/1176345636

Taniguchi M, Kakizawa Y (2000) Asymptotic Theory of Statistical Inference for Time Series. Springer New York, https://doi.org/10.1007/978-1-4612-1162-4

Whittle P (1953) Estimation and information in stationary time series. Ark Mat 2(5):423–434. https://doi.org/10.1007/BF02590998